



Contents lists available at ScienceDirect

Tunnelling and Underground Space Technology

journal homepage: www.elsevier.com/locate/tust

Impact of blasting parameters on vibration signal spectrum: Determination and statistical evidence

Ze-wei Wang^{a,*}, Xi-bing Li^a, Kang Peng^{b,a}, Jiang-feng Xie^{c,a}^a School of Resources and Safety Engineering, Central South University, Changsha 410083, China^b State Key Laboratory of Coal Mine Disaster Dynamics and Control, Chongqing University, Chongqing 400044, China^c LinTung-Yen & LiGuo-Hao Consultants Shanghai Ltd., Shanghai 200135, China

ARTICLE INFO

Article history:

Received 2 October 2014

Received in revised form 23 December 2014

Accepted 8 February 2015

Available online 14 March 2015

Keywords:

Blasting parameter

Vibration signal

Spectrum

K-means clustering

Student's *t*-test

ABSTRACT

Research on the impact of blasting parameters on vibration signals is of significant value for guiding blast-resistant design. Previous research was primarily aimed at the impact on vibration amplitude in the time domain but rarely focused on energy distribution in the frequency domain (i.e., spectrum). Based on large amounts of blast signals from a series of events, in this study, the primary parameters that affect the vibration spectrum were determined. First, the K-means method was used to cluster all of the signals into six distinct spectrum clusters. The *T* test was then utilized among different clusters, to detect discrepancies in continuous parameters, including total charge, maximum charge, concrete age and distance between the explosion source and measuring point. Meanwhile, a random clustering simulation was conducted to determine whether the other two discrete parameters, i.e., the number of detonator relays and the explosion source location, influence the spectrums of vibration signals. The results show that three of the six parameters studied have a close link to the vibration spectrum, whereas the other three do not. This study also discusses how the parameters impact the occurrence and evolution of vibration signals.

© 2015 Elsevier Ltd. All rights reserved.

1. Introduction

Vibration hazard, as an inevitable product of blasting, can have a considerable impact on the surrounding environment (Gorgulu et al., 2013). At present, studies on the factors influencing blasting vibration have been mainly aimed at the effect on vibration amplitude, such as peak particle velocity (PPV). Laws regulating blasting practice and scientific research into blast-induced ground vibrations use the PPV values as standard base parameters (Gorgulu et al., 2013). Site-specific empirical models for PPV are commonly used for blast-resistant designs (Amnieh et al., 2012; Xia et al., 2013; Ozer et al., 2013; Khandelwal and Singh, 2013). Related studies have emerged in large numbers in the past decades: on one hand, abundant improved empirical models were constantly proposed (Duvall and Petkof, 1959; Nicholls et al., 1971; Langefors and Kihlström, 1978; Pal Roy, 1991; Dey and Murthy, 2012; Kumar et al., 2014); on the other hand, various modern prediction

techniques, such as expert systems (Khandelwal and Singh, 2013), adaptive neuro-fuzzy inference systems (Ataei and Kamali, 2013) and fuzzy logic models (Ghasemi et al., 2013), were developed to improve the prediction of PPV. Also reported was the comparison of intelligence science techniques and empirical methods by Mohamadnejad et al. (2012). Compared with the attention paid to vibration amplitude, research about energy distribution in the frequency domain of blast vibration seems to be rarely reported. However, a shortage of current design code based on ground motion PPV alone has also been reported (Ma et al., 2002), which means that characteristics in the frequency domain should also be considered.

It is well known that blast vibrations induce a resonance in structures if the frequency of the ground vibration matches the natural frequency of the structure (Khandelwal and Singh, 2006) and that structural responses depend on the frequency of ground vibrations. Therefore, knowledge of how blasting parameters impact the frequency of vibration signals seems to be a potential source of guidance for environmentally friendly blast design. Among the few studies related to frequency, most treated the frequency feature of vibration as a single value (Khandelwal and Singh, 2006; Singh, 2002; Kahrman et al., 2006), such as dominant frequency. However, using a single value to represent the features in the frequency domain is definitely too simplified, as

* Corresponding author at: School of Resources and Safety Engineering, Central South University, Lushan South Road, Changsha 410083, China. Tel.: +86 15200858008.

E-mail addresses: wangzw.csu@gmail.com (Z.-w. Wang), xbli@mail.csu.edu.cn (X.-b. Li).

nonstationary blast-induced vibration contains a wealth of frequency components. For instance, high-frequency ground motion can cause brittle damage to structures (Lu et al., 2001; Wu et al., 2005), which may be ignored as the domain frequency is always much lower. Another example can be seen in BM-RI-8507, which tries to link PPV and dominant frequency to predict vibration damage. The data of the velocity–frequency–damage plots in this report shows sets of different damage levels are mixed together, with their boundaries difficult to determine. This may cause inconvenience in use and over conservative application. One possible reason for this may be the use of single frequency value. Therefore, rather than the dominant frequency value, this study considered the energy distribution in the frequency domain, i.e., the spectrum. Blasting parameters impacting the spectrum of vibration were determined and corresponding statistical evidence was given to begin to determine the relationship between blasting parameters and the vibration spectrum.

2. Background

2.1. Case description

The studied vibration signals were obtained from 35 blast events of Shizilong tunnel, which is a 1000 m long double-hole tunnel located at 28.116N, 112.744E (Fig. 1a). The width and height of the tunnel section is 16 m and 10.8 m, and the maximum burial depth is about 124 m. According to the geology report, the surrounding

rocks of north side of Shizilong tunnel are silt-slate and metasandstone with occurrence of $342^{\circ}\angle 63^{\circ}$, while those of the south side are sandstone and mudstone, with occurrence of $349^{\circ}\angle 21^{\circ}$.

Three-bench seven-step excavation method was used in this project, and the heights of the benches were 6.4 m, 2.4 m and 2 m from top to bottom (Fig. 1b). Boreholes were drilled horizontally with depth of 2.5 m. Emulsion explosive was used and the cartridge diameter was 32 mm. Blank column were remained at the bottom of boreholes, and the boreholes were sealed by stemming.

2.2. Blasting parameters

Many factors can affect blasting vibration, including geological structures (Caylak et al., 2014), blast design such as charges per delay, and geometry (USBM RI 8507). In this case, owing to the short period in which the vibration signals were measured (in a few days), the geology of each event can be considered as unchanged. This is also the case in terms of some design parameters, e.g., characteristics of drill holes, type of explosives as well as caps used. Therefore, six primary variable blasting parameters, incorporating aspects of energy, time and distance, were chosen in the study. They are:

- ELS – explosion source location;
- NRD – the number of relays of detonators;
- TC – total charge;

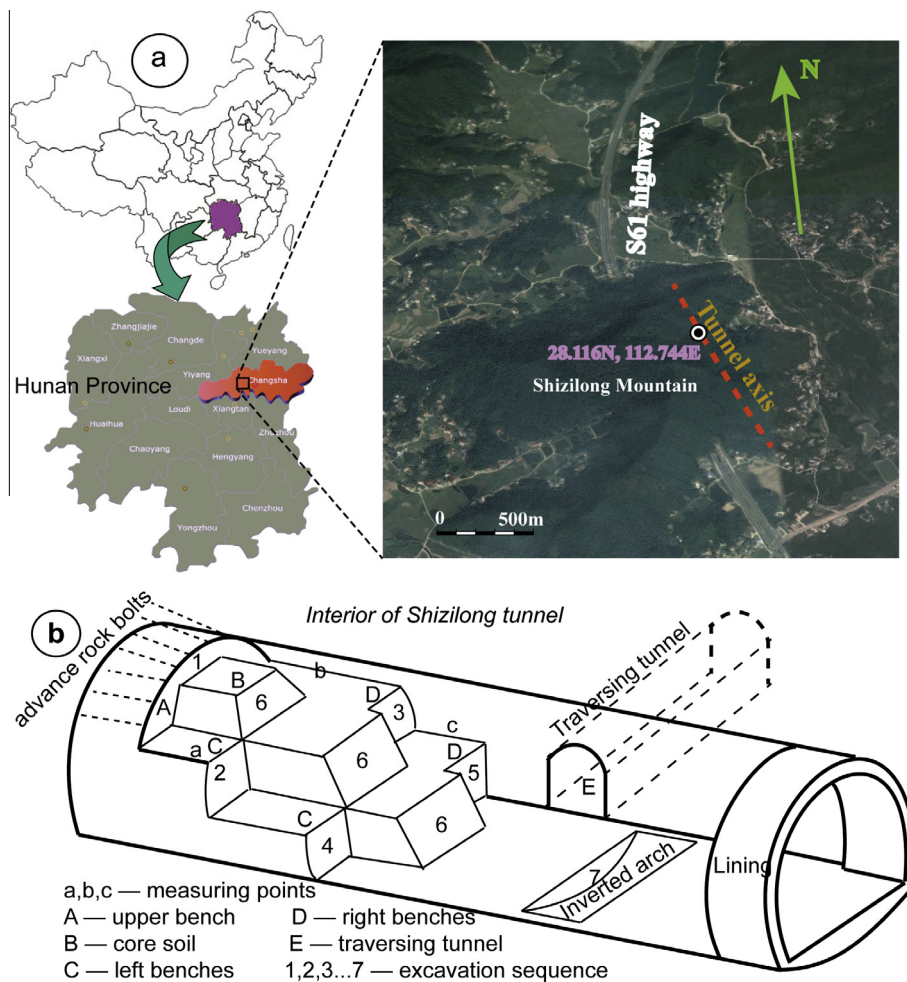


Fig. 1. Description of Shizilong tunnel: a – location; and b – inner structure of the tunnel.

MC – maximum charge of single detonation;
 CA – concrete age of measuring points;
 DSM – the distance between explosion source and a measuring point.

Among them, the first two were regarded as discrete parameters, while the rest were treated as continuous parameters (Appendix A). TC and MC ranged from several to tens of kilograms to match the practical demand. As the amount of charge indicates the energy of blast event, TC and MC were always considered in PPV empirical prediction expression (Nicholls et al., 1971; Ghosh and Daemen, 1983). DSM, another extremely important factor affecting vibration amplitude (Duvall and Fogelson, 1962), was calculated as the distance from the geometrical center of the explosion sources to the measuring point because of the scattering of multi-sources. The last continuous parameter was CA, which is of practical use for controlling the vibration of surrounding buildings under construction. A measuring point and the surrounding concrete are shown in Fig. 2.

Discrete parameters require a different method to determine whether the impact is significant. Therefore, ESL and NRD should be treated separately from the continuous parameters described above. ESL refers to the combination of explosion source location. AA from the ESL column in Appendix A, for instance, indicates that all the blast holes were located on the upper bench, while CD represents a left-right bench combination arrangement of blast holes. More details can be found in Fig. 1b. Another parameter is NRD, which indicates how the total energy is released. A small NRD denotes a concentrated release in time, while a large value denotes a relatively decentralized release.

3. Vibration signal clustering based on spectrum

As the six parameters exert a combined influence on the spectrum, it is difficult to determine the actual impact caused by each parameter separately. Hence, before a further study on the impact from each parameter, the vibration signals were classified into several distinct spectrum clusters; thus, the spectrums of the signals in each cluster are similar.

3.1. Similarity of spectrum

Although many powerful signal processing techniques were developed during the past decades, e.g., wavelet methods (Amiri and Asadi, 2009; Ling et al., 2005) and the Hilbert–Huang transform technique (Wang et al., 2013; Li et al., 2012), the Fourier transform is still a useful and effective tool for spectrum analysis. The discrete Fourier transform (DFT) was used for spectrum estimation in this study.

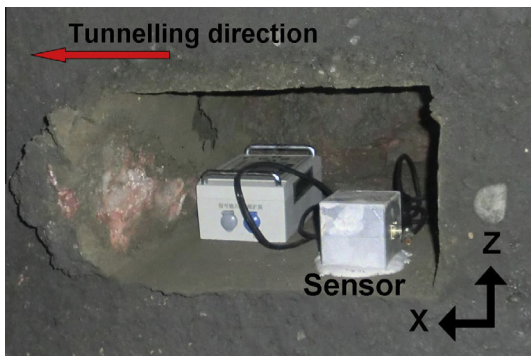


Fig. 2. Vibration sensor at measuring point c.

Each signal consists of three directional components, i.e., v_x, v_y, v_z . Apart from these three components, the absolute vibration amplitude is supplementarily defined as follows:

$$v_a = \sqrt{v_x^2 + v_y^2 + v_z^2} \quad (1)$$

Consider a real array $v = \{v_n | n = 0, 1, \dots, N-1\}$: v could be v_x, v_y, v_z or v_a . DFT transforms v to a new complex array $f = \{f_n | n = 0, 2, \dots, N-1\}$, in which

$$f_n = \sum_{k=0}^{N-1} v_k e^{-i\frac{2\pi}{N}kn}, \quad n = 0, 1, \dots, N-1 \quad (2)$$

The Fourier power spectrum $p = \{p_n | n = 0, 1, \dots, N-1\}$ is calculated as follows:

$$p_n = f_n \bar{f}_n, \quad n = 1, \dots, M \quad (3)$$

In this equation, \bar{f}_n represents the complex conjugate of f_n , while M makes Mf_s/N , in which f_s denotes the sample frequency, equal to the maximum frequency concerned, and the maximum frequency concerned could be predetermined as 500 Hz because the vast majority of energy is distributed at frequencies no greater than 500 Hz.

To obtain better performance in the following clustering, a new array called the cumulated power spectrum $c = \{c_n | n = 1, 2, \dots, M\}$ was defined as follows:

$$c_i = \frac{\sum_{k=1}^i p_k}{\sum_{k=1}^M p_k}, \quad i = 1, 2, \dots, M \quad (4)$$

The cumulated power spectrum is, in a sense, normalized to focus on the distribution of frequency rather than amplitude. Spectral distance, as a measurement of the spectral similarity between vibration signals i and j , was defined in Euclidean form:

$$d_{ij} = \sqrt{\sum_{k=1}^M (c_{k(i)} - c_{k(j)})^2} \quad (5)$$

3.2. K-means clustering

Cluster grouping based on large amounts of vibration signals is the key to the following study, and the next step is to determine the cluster analysis method. Adequate cluster methodologies are currently available, including the Hierarchical clustering method (Mirzaei and Rahmati, 2010), the K-means method (Jin et al., 2006) and intelligent algorithms such as the Ant Colony Algorithm (Ma and Tian, 2011), the ATTA method (Li et al., 2014), and others. The K-means method was chosen in this paper for its rapid convergence and advantageous stability. A brief description of K-means clustering is as follows:

- A. Determine the number of clusters K , and initialize the K cluster centers. K vibration signals can be randomly picked here as the initialized cluster centers.
- B. Traverse all the signals. Each vibration signal is classified as part of the cluster surrounding its closest cluster center.
- C. Update centers. The average cumulated power spectrum of all signals in a cluster is taken as the new cluster center.
- D. Repeat B and C until all the centers remain stable, and the clustering is complete.

After several trials, $K = 6$ was selected as the best cluster number. The six cluster centers of the cumulated power spectrum are illustrated in Fig. 3.

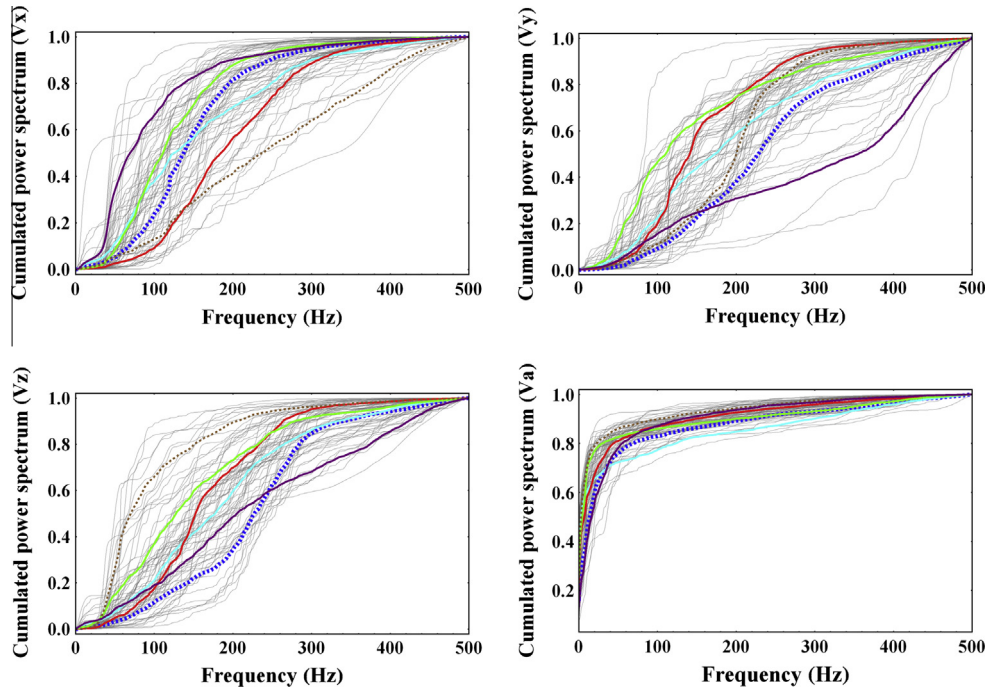


Fig. 3. Cluster centers of vibration signals iterated by K-mean method: v_x , v_y , v_z and v_a .

4. Demonstration of impact on vibration spectrum from blasting parameters

4.1. Continuous parameters

The continuous parameters include TC, MC, CA, and DSM. Generally speaking, if a continuous parameter made a difference in the spectrums of vibration signals, the spectrums should in turn reflect this parameter. Therefore, signals with similar spectrums should have similar parameter values, while the parameter values of signals in different clusters should be discrepant. Hence, the two-sample Student’s *t*-test was utilized to detect the discrepancy.

The *p*-value in Student’s *t*-test is known as the error probability of the hypothesis that the means of the two samples tested are different. In other words, a small *p*-value suggests that it is likely that a discrepancy exists between the means of the two samples. Student’s *t*-test was applied between every pair of clusters obtained in Section 3.2, and the results for the *x*-direction component are displayed in Table 1 (the results of the other components exhibited similar features to the *x*-direction component and are therefore not shown here). The average *p*-values of each blasting parameter and each component are also calculated and are shown in Table 2.

Table 1
The *p*-values between each pair of clusters of *x*-direction signals.

		C2	C3	C4	C5	C6		C2	C3	C4	C5	C6
C1	TC (avg: 0.641)	0.728	0.666	0.887	0.564	0.914	MC (avg: 0.706)	0.978	0.743	0.905	0.397	0.689
C2		–	0.406	0.810	0.330	0.600		–	0.767	0.928	0.426	0.710
C3			–	0.488	0.820	0.694			–	0.818	0.492	0.945
C4				–	0.368	0.771				–	0.402	0.768
C5					–	0.568					–	0.624
C1	CA (avg: 0.330)	0.010	0.027	0.101	0.076	0.004	DSM (avg: 0.259)	0.173	0.078	0.454	0.196	0.461
C2			0.784	0.159	0.340	0.901			0.534	0.443	0.001	0.316
C3				0.295	0.523	0.678				0.187	0.000	0.100
C4					0.704	0.098					0.014	0.920
C5						0.248						0.006

Table 2
Average *p*-values of each blasting parameter.

Blasting parameters	v_x	v_y	v_z	v_a
TC	0.641	0.605	0.397	0.584
MC	0.706	0.538	0.393	0.609
CA	0.330	0.301	0.361	0.351
DSM	0.259	0.162	0.206	0.242

As shown in Table 1, the *p*-values of TC stay at a high level: only a few of them are 0.5 or lower. Similar features can be observed for MC, which is another energy parameter. The *p*-values of CA and DSM, however, show a relatively low level compared with TC and MC. Table 2 displays those features clearly in general: all of the average *p*-values of TC and MC remain above 0.5 expect for the *z*-direction, while the average *p*-values of CA remain at a level no more than 0.4, and DSM, even lower, no more than 0.3. This result suggests that TC and MC may barely affect the spectrum of the vibration signal, while CA and DSM have a comparatively significant effect on it. At least, it can be inferred that CA and DSM exert a more important influence on the spectrum of the vibration signal than TC and MC.

4.2. Discrete parameters

All the signals can be separated into several groups according to NRD, such that signals in the same group have the same NRD. Similarly, the studied samples can also be divided into groups of AA, BB, CC, DD, EE and so on according to ELS. Continuing the basic idea in the previous section, if a discrete parameter exerts a significant effect on spectrum, there should be a similarity between the grouping based on the parameter and the grouping based on spectrum. Here, a similarity index $S(A, B)$, was identified to measure the similarity. Consider, for example, grouping $A = \{\{a, b, c, d\}, \{e, f, g\}\}$ and grouping $B = \{\{a, b\}, \{c, d, e, f, g\}\}$. If elements c and d are transferred from the first group to the second in grouping A , with the remaining five elements staying in place, then grouping A transforms to B . Thus, the similarity index $S(A, B) = 5$. The similarity indexes between the groupings based on spectrum and the groupings based on NRD and ELS were calculated as follows:

$$\{S_x(\text{NRD, SPCT}), S_y(\text{NRD, SPCT}), S_z(\text{NRD, SPCT}), S_a(\text{NRD, SPCT})\} = \{23, 23, 28, 28\}$$

$$\{S_x(\text{ELS, SPCT}), S_y(\text{ELS, SPCT}), S_z(\text{ELS, SPCT}), S_a(\text{ELS, SPCT})\} = \{21, 23, 28, 22\}$$

It is difficult to say whether there is significant similarity or based on the similarity index directly. For this reason, a supplementary random clustering simulation was conducted to interpret the similarity level:

- A. Fit the distribution models of the distances identified by Eq. (5). The fitting result is shown in Fig. 4.
- B. Based on the fitted distribution models in step A, regenerate the distance matrix of all the signals randomly.
- C. Cluster the signals into groups according to the regenerated distance matrix, and calculate the similarity index S between the new grouping and the groupings based on NRD and ELS, respectively.
- D. Repeat B and C 3000 times to obtain the distribution of S , which is illustrated in Fig. 5.

Fig. 5 also displays the similarity indexes between groupings of discrete parameters and the grouping of the spectrums. From the figure, it can be observed that it is unlikely for the similarity index to be greater than or equal to 23 in the random clustering simulation (with a probability of less than 10% totally). However, the similarity indexes between the grouping of NRD and of the spectrum, with two of them equal to 23 and the other two equal to

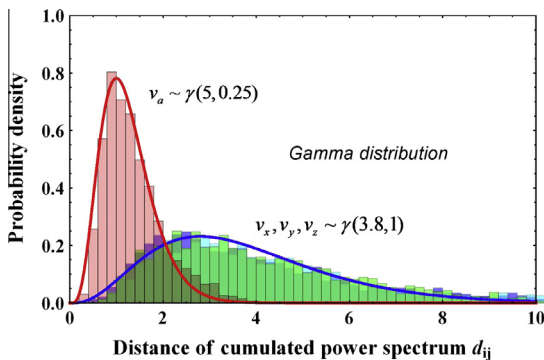


Fig. 4. Distribution of signal spectrum distance: gamma distribution model was used.

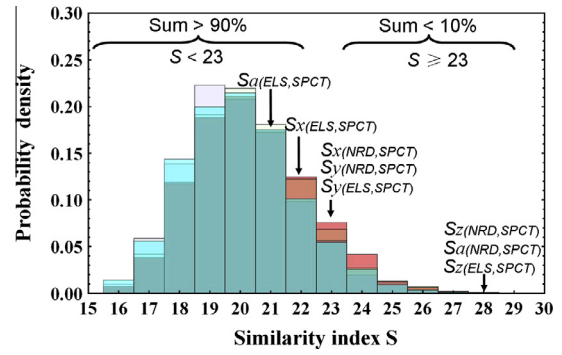


Fig. 5. Distribution of similarity index obtained by random clustering simulation.

28, seemed to remain at a higher level than expected by chance. With regard to ELS, it seemed less obvious that the similarity indexes had a distinct difference from random clustering simulation. The result indicates that NRD affects spectrum, whereas the evidence that ELS influences the spectrum is not obvious.

5. Discussion

This study, as reported in previous sections, shows statistical evidence that NRD, CA, and DSM affect the spectrum of vibration signals, but any such influence is less apparent with regard to TC, MC and ELS. Further discussion, categorizing the six parameters into aspects of energy, space and time, is as follows.

Although TC and MC govern the amplitude of vibration, the two energy parameters seem to have little influence on the spectrum of blast induced vibration in this study; therefore, the roles of TC and MC to vibration is something similar to “amplitude scaler”, which can only amplify the amplitude but not change the energy distribution in the frequency domain.

DSM represents the relative position between explosion sources and measuring points, while ELS can only reflect the spatial position of the explosion sources. The effect of DSM may be caused by the natural filtering function of rock mass. That is to say, the longer the vibration wave propagates, the greater the filtering action. The ELS result may be caused by the irrationality in defining ELS in the study.

It is well known that NRD determines the vibration waveform in the time domain; meanwhile, this study found that NRD also exhibits a great effect on energy distribution in the frequency domain. Hence, it can be inferred that NRD controls the features of vibration fundamentally in both the time domain and the frequency domain. Another time parameter impacting the spectrum of vibration signals is CA, which may alter the spectrum by changing the physical and mechanical properties of material at the measuring points.

Based on the previous discussion, Fig. 6 presents the occurrence and evolution of vibration signals and shows the periods that blasting parameters contribute to altering signals.

Further study should focus on establishing the relation between NRD, DSM and CA with the vibration spectrum, thus to predict spectrums and to serve blast design. However, unlike the prediction of PPV, the spectrum of a vibration signal is not a single value but a frequency series, thereby traditional regression methods for predictions of single dependent variable problem are no longer suitable for this study. The first important step for predicting spectrum is to reduce the dimensions of the spectrum. A good dimension reduction algorithm should not only be able to transform the multidimensional spectrum to a small number of variables

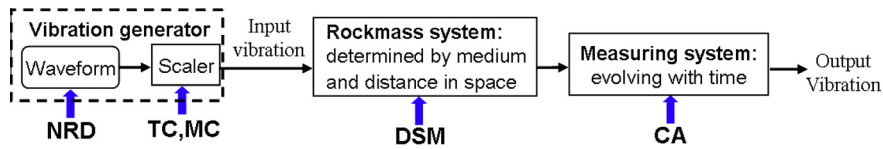


Fig. 6. The occurrence and evolution of vibration signals: parameters impact vibration in different period.

efficiently, but also remain the basic feature of the spectrum. In fact, replacing the spectrum with the dominant frequency is also a dimension reduction method, although the dominant frequency may only reflect few characteristic of the spectrum. The authors think modeling the spectrum using parameterized models is a potential alternative to reduce the spectrum dimension. Thus, the prediction of spectrum is transferred to the prediction of a few parameters used in the models. However, this still remains an uncompleted task before a series of detailed problems are solved in further researches.

6. Conclusions

A series of mathematical methods, including clustering analysis, Student’s *t*-test and random clustering simulation, were used to unearth the information carried by vibration signals. Conclusions are as follows:

Student’s *t*-test indicates that DSM and CA exert a significant effect on the spectrum of the vibration signal, whereas TC and MC may only affect the amplitude in the time domain. Random clustering simulation shows that apart from the effect on waveform in the time domain, NRD also govern spectrums of vibration signals. The evidence that ELS affects the vibration spectrum remains unclear. From further discussion, it can be inferred that NRD, TC and MC influence signals when vibrations are generated, and DSM influences the vibration spectrum through the filter function of the rockmass system when vibration waves propagate in the rockmass. CA eventually determines the spectrum of the measured signals.

Acknowledgement

The authors would like to acknowledge the financial supports from the National Natural Science Foundation of China (Nos. 41272304 and 11472311).

Appendix A

Blasting parameters of vibration signals.

Signal number	NRD	ELS	TC	MC	CA	DSM	Delay steps used
			(kg)	(kg)	(h)	(m)	
1	1	DD	5	5	30	6.4	1
2	2	EE	8.4	6	32	17.7	3, 5
3	7	AA	114	45.6	41	41.4	1, 3, 5, 7, 9, 11, 13
4	2	BB	11	7	83	8.3	5, 7
5	7	AA	72	28.8	109	10.9	1, 3, 5, 7, 9, 11, 13
6	4	DE	42	22	10	39.2	1, 3, 5, 7
7	3	DD	14.7	7	130	31.1	3, 5, 7
8	7	AA	68	13	139	12.4	1, 3, 5, 7, 9, 11, 13

Appendix A (continued)

Signal number	NRD	ELS	TC	MC	CA	DSM	Delay steps used
			(kg)	(kg)	(h)	(m)	
9	4	EE	32	13	167	41.3	9, 11, 13, 15
10	2	EE	4.6	3.8	168	41.3	11, 13
11	2	AD	68	23	170	21.6	11, 13
12	3	DD	29.8	14.6	192	25.8	3, 5, 7
13	4	EE	30.9	11.9	194	42.8	9, 11, 13, 15
14	2	AA	11	6.6	206.5	15.7	9, 11
15	3	DD	16	6	210	21.38	3, 5, 7
16	3	CC	8	4	230	23.1	3, 5, 7
17	7	AA	108	43.2	12	8.4	1, 3, 5, 7, 9, 11, 13
18	3	AA	10	3.6	254	16.7	5, 7, 9
19	3	EE	44	20	257	44.4	9, 11, 13
20	2	EE	12	8	258	44.4	11, 13
21	4	EE	28	8	282	45.9	1, 3, 5, 7
22	3	AA	10	5	282.3	18.4	5, 7, 9
23	2	EE	10	7.8	282.5	45.9	11, 13
24	4	EE	30	10	301	47.2	9, 11, 13, 15
25	1	CD	10	10	322.5	17.7	7
26	4	AA	6.4	2	348	19.8	3, 5, 7, 9
28	3	CD	10	5.8	353	12.2	7
27	3	AA	6.6	2.4	18	12.5	1, 5, 9
29	3	DD	64	32	372.5	12.5	7, 9, 11
30	6	AA	8	3	396	21.6	1, 3, 5, 7, 9, 11
31	4	DD	21.2	7.2	404	9.8	5, 7, 9, 11
32	3	CC	24	12	417	15.8	3, 5, 7
33	2	CC	6	5	440	17	3, 5
34	1	DD	5	5	30	32	1
35	2	EE	8.4	6	32	39.2	3, 5
36	7	AA	114	45.6	41	8.8	1, 3, 5, 7, 9, 11, 13
37	3	DD	12.2	4.8	44	29.2	3, 5, 7
38	3	BB	12	6	46	8.3	5, 9, 13
39	3	CE	41.4	22	65	36	1, 3, 5
40	2	BB	11	7	119	8.4	5, 7
41	7	AA	72	28.8	145	11.5	1, 3, 5, 7, 9, 11, 13
42	3	DD	14.7	7	166	33	3, 5, 7
43	7	AA	68	13	175	13.1	1, 3, 5, 7, 9, 11, 13
44	4	EE	32	13	203	31.4	9, 11, 13, 15
45	2	EE	4.6	3.8	204	31.4	11, 13
46	3	AD	68	23	206	24.6	5, 7, 9
47	3	DD	29.8	14.6	228	29.7	3, 5, 7
48	4	EE	30.9	11.9	230	32.5	9, 11, 13,

(continued on next page)

Appendix A (continued)

Signal number	NRD	ELS	TC	MC	CA	DSM	Delay steps used
			(kg)	(kg)	(h)	(m)	
							15
49	2	AA	11	6.6	242.5	16.5	9, 11
50	3	DD	16	6	246	24.5	3, 5, 7
51	3	CC	8	4	266	18	3, 5, 7
52	3	AA	10	3.6	290	17.5	5, 7, 9
53	3	EE	44	20	293	33.5	9, 11, 13
54	2	EE	12	8	294	33.5	11, 13
55	4	EE	28	8	318	34.5	1, 3, 5, 7
56	3	AA	10	5	318.3	19.3	5, 7, 9
57	2	EE	10	7.8	318.5	34.5	11, 13
58	4	EE	30	10	337	35.4	9, 11, 13, 15
59	1	CD	10	10	358.5	18.8	7
60	4	AA	6.4	2	384	20.7	3, 5, 7, 9
61	3	CD	10	5.8	389	14.9	7
62	3	DD	64	32	408.5	17.2	7, 9, 11
63	6	AA	8	3	432	22.5	1, 3, 5, 7, 9, 11
64	4	DD	21.2	7.2	440	15.6	5, 7, 9, 11
65	3	CC	24	12	453	7.8	3, 5, 7
66	3	DD	12.2	4.8	80	31.3	3, 5, 7
67	3	BB	12	6	82	8.3	5, 9, 13
68	3	CE	41.4	22	101	17	3, 5, 7

ELS – explosion source location; NRD – number of the relays of detonators; TC – total charge; MC – maximum charge of single detonation; CA – concrete age of measuring points; DSM – the distance between explosion source and a measuring point.

References

- Amiri, G.G., Asadi, A., 2009. Comparison of different methods of wavelet and wavelet packet transform in processing ground motion records. *Int. J. Civil Eng.* 7, 248–257.
- Amnieh, H.B., Siamaki, A., Soltani, S., 2012. Design of blasting pattern in proportion to the peak particle velocity (PPV): artificial neural networks approach. *Saf. Sci.* 50, 1913–1916.
- Ataei, M., Kamali, M., 2013. Prediction of blast-induced vibration by adaptive neuro-fuzzy inference system in Karoun 3 power plant and dam. *J. Vib. Control* 19, 1906–1914.
- Caylak, C., Kocaslan, A., Gorgulu, K., Buyuksarac, A., Arpaz, E., 2014. Importance of ground properties in the relationship of ground vibration–structural hazard and land application. *J. Appl. Geophys.* 104, 6–16.
- Dey, K., Murthy, V.M.S.R., 2012. Prediction of blast-induced overbreak from uncontrolled burn-cut blasting in tunnels driven through medium rock class. *Tunnelling Underground Space Technol.* 28, 49–56.
- Duvall, W.I., Fogelson, D.E. 1962. Review of criteria for estimating damage to residences from blasting vibrations (No. BM-RI-5968). In: M.U. (Ed.), Bureau of Mines College Park.
- Duvall, W.I., Petkof, B. 1959. Spherical propagation of explosion-generated strain pulses (U). Report of investigation. US Bureau of Mines, Pittsburgh, pp. 5483–5521.
- Ghasemi, E., Ataei, M., Hashemolhosseini, H., 2013. Development of a fuzzy model for predicting ground vibration caused by rock blasting in surface mining. *J. Vib. Control* 19, 755–770.
- Ghosh, A., Daemen, J.J. 1983. A simple new blast vibration predictor (based on wave propagation laws). In: Association, A.R.M. (Ed.), The 24th US Symposium on Rock Mechanics (USRMS), Texas, USA, pp. 151–161.
- Gorgulu, K., Arpaz, E., Demirci, A., Kocaslan, A., Dilmac, M.K., Yuksek, A.G., 2013. Investigation of blast-induced ground vibrations in the Tulu boron open pit mine. *Bull. Eng. Geol. Environ.* 72, 555–564.
- Jin, R.M., Goswami, A., Agrawal, G., 2006. Fast and exact out-of-core and distributed k-means clustering. *Knowl. Inf. Syst.* 10, 17–40.
- Kahriman, A., Ozer, U., Aksoy, M., Karadogan, A., Tuncer, G., 2006. Environmental impacts of bench blasting at Hisarcik Boron open pit mine in Turkey. *Environ. Geol.* 50, 1015–1023.
- Khandelwal, M., Singh, T.N., 2006. Prediction of blast induced ground vibrations and frequency in opencast mine: a neural network approach. *J. Sound Vib.* 289, 711–725.
- Khandelwal, M., Singh, T.N., 2013. Application of an expert system to predict maximum explosive charge used per delay in surface mining. *Rock Mech. Rock Eng.* 46, 1551–1558.
- Kumar, R., Choudhury, D., Bhargava, K., 2014. Prediction of blast-induced vibration parameters for soil sites. *Int. J. Geomech.*, 14
- Langefors, U., Kihlström, B., 1978. The Modern Technique of Rock Blasting. Wiley.
- Li, L.F., Li, X.B., Ma, H.P., Xie, J.F., 2012. Blast-induced cumulative effects in surrounding rock of Largespan tunnel under multiple blasts. *Adv. Mater. Res.* 378, 498–501.
- Li, X.B., Wang, Z.W., Peng, K., Liu, Z.X., 2014. Ant colony ATTA clustering algorithm of rock mass structural plane in groups. *J. Cent. South Univ.* 21, 709–714.
- Ling, T.H., Li, X.B., Dai, T.G., Peng, Z.B., 2005. Features of energy distribution for blast vibration signals based on wavelet packet decomposition. *J. Cent. South Univ. Technol.* 12, 135–140.
- Lu, Y., Hao, H., Ma, G.W., Zhou, Y.X., 2001. Simulation of structural response under high-frequency ground excitation. *Earthquake Eng. Struct.* 30, 307–325.
- Ma, G.W., Hao, H., Lu, Y., Zhou, Y.X., 2002. Distributed structural damage generated by high-frequency ground motion. *J. Struct. Eng.-ASCE* 128, 390–399.
- Ma, J.H., Tian, F.Z., 2011. Intelligent learning ant colony algorithm. *Appl. Mech. Mater.* 48–49, 625–631.
- Mirzaei, A., Rahmati, M., 2010. A novel hierarchical-clustering-combination scheme based on fuzzy-similarity relations. *IEEE Trans. Fuzzy Syst.* 18, 27–39.
- Mohamadnejad, M., Gholami, R., Ataei, M., 2012. Comparison of intelligence science techniques and empirical methods for prediction of blasting vibrations. *Tunnelling Underground Space Technol.* 28, 238–244.
- Nicholls, H.R., Johnson, C.F., Duvall, W.I., 1971. Blasting Vibrations and Their Effects on Structures. US Government Printers.
- Ozer, U., Karadogan, A., Kahriman, A., Aksoy, M., 2013. Bench blasting design based on site-specific attenuation formula in a quarry. *Arab. J. Geosci.* 6, 711–721.
- Pal Roy, P., 1991. Vibration control in an opencast mine based on improved blast vibration predictors. *Mining Sci. Technol.* 12, 157–165.
- Singh, P.K., 2002. Blast vibration damage to underground coal mines from adjacent open-pit blasting. *Int. J. Rock Mech. Min.* 39, 959–973.
- Stagg, M.S., Kopp, J.W., Dowding, C.H., 1980. Structure Response and Damage Produced by Ground Vibrations from Surface Blasting (No. BM-RI-8507). US Bureau of Mines, Washington, DC.
- Wang, Z.Y., Fang, C., Chen, Y.L., Cheng, W.F., 2013. A comparative study of delay time identification by vibration energy analysis in millisecond blasting. *Int. J. Rock Mech. Min.* 60, 389–400.
- Wu, C.Q., Hao, H., Lu, Y., 2005. Dynamic response and damage analysis of masonry structures and masonry infilled RC frames to blast ground motion. *Eng. Struct.* 27, 323–333.
- Xia, X., Li, H.B., Li, J.C., Liu, B., Yu, C., 2013. A case study on rock damage prediction and control method for underground tunnels subjected to adjacent excavation blasting. *Tunnelling Underground Space Technol.* 35, 1–7.